16.52% Efficiency All-Polymer Solar Cells with High Tolerance of the Photoactive Layer Thickness

Wenqing Zhang, Chenkai Sun, Indunil Angunawela, Lei Meng, Shucheng Qin, Liuyang Zhou, Shaman Li, Hongmei Zhuo, Guang Yang, Zhi-Guo Zhang, Harald Ade*, and Yongfang Li**

W. Zhang, Dr. C. Sun, Prof. G. Yang,

College of Chemistry, and Green Catalysis Center, Zhengzhou University, Zhengzhou 450001, China

E-mail: schenkai@zzu.edu.cn

Dr. L. Meng, S. Qin, L. Zhou, H. Zhuo, Prof. Y. Li,

Beijing National Laboratory for Molecular Sciences, CAS Key Laboratory of Organic Solids, Institute of Chemistry, Chinese Academy of Sciences, Beijing 100190, China

E-mail: liyf@iccas.ac.cn

Dr. L. Meng, S. Qin, L. Zhou, S. Li, H. Zhuo, Prof. Y. Li,

School of Chemical Science, University of Chinese Academy of Sciences, Beijing 100049, China

I. Angunawela, Prof. H. Ade,

Department of Physics and Organic and Carbon Electronics Laboratories (ORaCEL), North Carolina State University, Raleigh, NC, USA

E-mail: hwade@ncsu.edu

Prof. Y. Li,

Laboratory of Advanced Optoelectronic Materials, Suzhou Key Laboratory of Novel Semiconductor-Optoelectronics Materials and Devices, College of Chemistry, Chemical Engineering and Materials Science, Soochow University, Suzhou 215123, China

This is the author manuscript accepted for publication and has undergone full peer review but has not been through the copyediting, typesetting, pagination and proofreading process, which may lead to differences between this version and the Version of Record. Please cite this article as doi: 10.1002/adma.202108749.

Prof. Z.-G. Zhang,

State Key Laboratory of Organic/Inorganic Composites, Beijing University of Chemical Technology, Beijing 100029, China

Keywords: all-polymer solar cells; PTQ10 as third component; morphology control; energy level matching; high tolerance of the photoactive layer thickness.

All-polymer solar cells (all-PSCs) have drawn growing attentions and achieved tremendous progresses recently, but its power conversion efficiency (PCE) still lags behind the small molecule acceptor (SMA)-based PSCs due to the relative difficulty on morphology control of the polymer photoactive blends. Here, we introduce our low-cost PTQ10 as the second polymer donor (the third component) into the PM6:PY-IT blend to finely tune energy level matching and microscopic morphology of the polymer blend photoactive layer. The addition of PTQ10 decreases the π-π stacking distance, and increases the π-π stacking coherence length and the ordered face-on molecular packing orientation, which improves charge separation and transport in the photoactive layer. Moreover, deeper highest occupied molecular orbital energy level of the polymer donor PTQ10 than PM6 leads to higher open-circuit voltage of the ternary all-PSCs. As a result, a PCE of 16.52% is achieved for the ternary all-PSCs, which is one of the highest PCEs for all-PSCs. In addition, the ternary devices exhibit high tolerance of the photoactive layer thickness with high PCEs of 15.27% and 13.91% at photoactive layer thickness of ~ 205 nm and ~ 306 nm respectively, which are the highest PCEs so far for the all-PSCs with thick photoactive layer.

1. Introduction

All-polymer solar cells (all-PSCs), utilizing a polymer blend photoactive layer with a *p*-type conjugated polymer as electron donor and an *n*-type conjugated polymer as electron acceptor, have attracted growing research interests in recent years, due to their advantages of good solution processability, outstanding mechanical flexibility, and excellent morphological stability.[1-7] Power conversion efficiency (PCE) of the state-of-the-art all-PSCs has reached over 15~17% currently,[8-14] mainly benefited from the recent development of the high performance polymer acceptors of "polymerized small molecule acceptors" (PSMAs). Nonetheless, PCE of the all-PSCs still lags behind that (over 18%) of the small molecule acceptor (SMA)-based PSCs (based on *p*-type conjugated polymer as electron donor and *n*-type small molecule as electron acceptor) because of the relative difficulty on finely tuning microscopic morphology of the all-polymer blends.[15-18]

To obtain high performance *n*-type polymer acceptors, Zhang *et al.* proposed the "polymerizing small molecule acceptor" strategy in 2017, and synthesized a narrow bandgap PSMA PZ1 by copolymerizing the SMA IDIC-C16 with the aromatic thiophene linking unit,[19] in considering the features of broad and strong light absorption in the near infrared (NIR) region, easily tunable electronic energy levels, and high morphology controllability of the SMAs. In 2019, Meng *et al.* reported a 11.2% efficiency all-PSC by using PZ1 as acceptor and the classic polymer PM6 as donor.[20] After that, the "polymerizing small molecule acceptor" strategy has received great attention,[21] and a large number of highly efficient PSMAs are developed. For instance, Yao *et al.* designed and synthesized a narrow bandgap PSMA PFBDT-IDTIC by replacing the thiophene unit in the backbone of PZ1 with the two-dimensional conjugated benzodithiophene unit, and reported a high performance all-PSC with PCE of 10.3%.[22] In addition, encouraged by the excellent photovoltaic performance of the A-DA'D-A structured SMA Y6,[23] several research groups reported Y6 derivatives based high performance PSMAs, and increased PCEs of the all-PSCs to 12~16%.[6,24-29] For example, Jia *et al.* synthesized a Y6 derivatives based PSMA PJ1, and achieved a high PCE of 14.4% by using

polymer PBDB-T as donor in 2020.[24] Sun *et al.* developed a narrow bandgap PSMA L14 with an acceptor-acceptor (A-A) type backbone by copolymerizing the Y6 derivative with the bithiophene imide unit, and reported a 14.3% efficiency all-PSC.[26] Luo *et al.* designed and synthesized a regioregular PSMA PY-IT by precisely controlling the positions of Br atoms (act as polymerization sites) on the end groups of the SMA building block, and demonstrated an excellent PCE of 15.05% when blending it with the polymer donor PM6.[27] Very recently, Du *et al.* designed and synthesized a PSMA PN-Se with a Y18 derivative as main building block and selenophene as linking unit, and achieved a highly efficient all-PSC with PCE of 16.16%.[29]

Morphology of the photovoltaic layer significantly affects the photovoltaic properties of the all-PSCs. Compared with the SMAs-based PSCs, morphology control of the photoactive layer of all-PSCs is relatively difficult due to the long conjugated molecular backbone and large moelcular weight of the polymer acceptors.[1,2,30-32] Therefore, achieving suitable nano-scale interpenetrating network photoactive layer with ordered molecular stacking and favourable molecular orientation is crucial for high performance all-PSCs. Regarding the morphology control of the photoactive layer, the utilization of additives, especially solvent additives such as 1-chloronaphthalene (CN) and 1,8-diiodooctane (DIO), has proven to be an effective approach to address the problem.[33-38] For instance, Liu *et al.* reported that the addition of the DIO additive could result in more favorable phase separation and domain size for the J71:N2200 blend photoactive layer, thus obtaining higher fill factor (FF) and PCE of the corresponding all-PSCs, compared with that of the device without DIO additive.[38] In addition, adding the third polymer component (either polymer donor or polymer acceptor) into the host blends is also a practical approach to finely tune the morphology of the photoactive layer of all-PSCs.[9,11,39-41] For instance, Liu *et al.* added a small amount of polymer acceptor BN-T into the PM6:PY-IT blend to regulate the molecular crystallinity and phase separation of the photoactive layer, and promoted the PCE of the ternary device (PM6:PY-IT:BN-T) to 16.09%

from 15.11% (PM6:PY-IT).[41] Recently, Sun *et al.* developed two regioregular PSMAs, L15 and MBTI, and reported a 15.2% efficiency binary all-PSC by using L15 as acceptor and polymer PM6 as donor. Then, they introduced MBTI as a guest into the PM6:L15 host system to modify morphology of the photoactive layer, and an impressive ternary all-PSC with PCE of 16.2% was achieved.[9] Yu *et al.* reported a difluoro-monobromo substituted end group, and then constructed a high performance PSMA PY2F-T which yielded an outstanding all-PSC with PCE of 15.22% when using the polymer PM6 as donor.[10] Then, Sun *et al.* introduced the second polymer acceptor PY-T into the PM6:PY2F-T blend to finely tune the microstructures of the photoactive layer, and they achieved a 17.2% efficiency ternary all-PSC, which is the highest PCE of the all-PSCs currently.[11]

In order to further boost the photovoltaic performance of the all-PSCs, here we introduce our low cost polymer donor PTQ10[42] as the second polymer donor (or the third component) into the PM6:PY-IT blend (molecular structures of PM6, PTQ10, and PY-IT are shown in **Figure 1a**) to subtly regulate the microscopic morphology of the photoactive layer. The addition of PTQ10 induces a change in molecular packing with the decreased π-π stacking distance, increased π-π stacking coherence length (CL), and more ordered face-on molecular packing orientation in the vertical direction of substrate, which leads to improved exciton dissociation, reduced charge carrier recombination, and better charge transport capability (higher charge mobilities) of the devices. Moreover, the deeper highest occupied molecular orbital (HOMO) energy level of PTQ10 compared to PM6 leads to increased open-circuit voltage (V_{oc}) of the ternary device. As a result, benefiting from the simultaneously enhanced V_{oc}, short-circuit current density (J_{sc}), and FF, the PM6:PTQ10:PY-IT based ternary all-PSC demonstrates an outstanding PCE of 16.52% which is one of the highest PCEs for all-PSCs so far. Meanwhile, photovoltaic performance of the ternary devices exhibits excellent tolerance of the photoactive layer thickness ranging from ~ 70 to ~ 300 nm. The devices display high PCEs of 15.27% and 13.91% at photoactive layer thickness of ~205 nm and ~306 nm

respectively, which are the highest PCEs, so far for all-PSCs with the thick photoactive layer (>150 nm). This work demonstrates the importance of ternary blend strategy for improving the photovoltaic performance of the all-PSCs, and suggests the great potential of PM6:PTQ10:PY-IT based ternary all-PSCs in future industrial application.

2. Results and Discussion

Molecular structures of the polymer donors PTQ10 and PM6,[43] and polymer acceptor PY-IT are depicted in **Figure 1a**. These three polymers exhibit good solubility in common organic solvents at room temperature. The UV-vis absorption spectra of the three polymers in their neat films are shown in **Figure 1b**. The two polymer donors (PTQ10 and PM6) show strong light absorption peak in the wavelength range of 470 to 620 nm, which is complementary with the absorption peak (630 to 860 nm) of the polymer acceptor PY-IT. **Figure 1c** shows the absorption spectra of the polymer blend films. It is worth noting that, compared with the PM6:PY-IT (1.2:1.0, w/w) binary blend, the PM6:PTQ10:PY-IT (1.0:0.2:1.0, w/w/w) ternary blend exhibits slightly red-shifted absorption edge, implying that adding a small amount of PTQ10 into the PM6:PY-IT blend could induce molecular aggregation of the polymer acceptor.

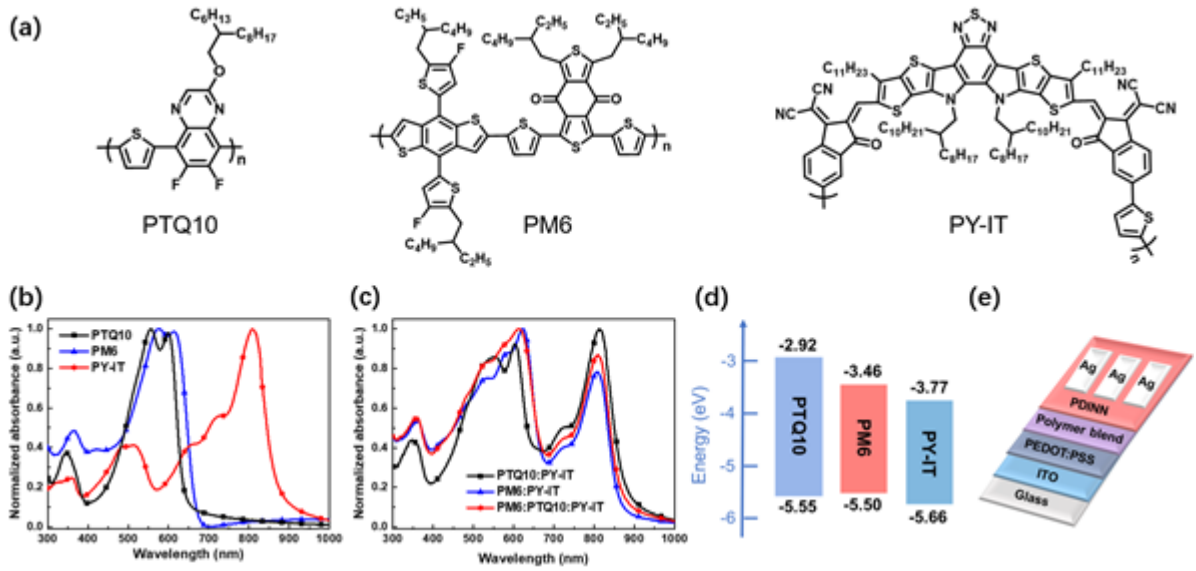

Figure 1. a) Molecular structures and b) normalized film absorption spectra of the polymer donors PTQ10, PM6, and polymer acceptor PY-IT. c) Normalized film absorption spectra of the polymer blend films. d) Electronic energy level diagrams of PTQ10, PM6, and PY-IT. e) Device architecture of the all-PSCs used in this work.

The electronic energy levels of the three polymers are measured by electrochemical cyclic voltammetry (as shown in **Figure S1** in the Supporting Information (SI)). Their E_{HOMO}/E_{LUMO} are calculated from the onset oxidation and onset reduction potentials ($\varphi_{ox}/\varphi_{red}$) according to the equation of E_{HOMO}/E_{LUMO} = -e ($\varphi_{ox}/\varphi_{red}$ + 4.8 - $\varphi_{Fc/Fc+}$) (eV), where the $\varphi_{Fc/Fc+}$ (internal reference) is measured to be 0.47 V versus Ag/AgCl reference electrode. The E_{HOMO}/E_{LUMO} values of PTQ10, PM6, and PY-IT are calculated to be -5.55/-2.92 eV, -5.50/-3.46 eV, and -5.66/-3.77 eV, respectively. The electronic energy levels of the three polymers are summarized in **Figure 1d.**

To investigate the effect of the addition of the third polymer component PTQ10 on photovoltaic properties of the devices, the binary and ternary all-PSCs are fabricated with traditional device architectures of ITO/PEDOT:PSS (poly(3,4-ethylenedioxythiophene):poly(styrene-sulfonate))/Photoactive layer/PDINN (aliphatic amine-functionalized perylene-diimide)/Ag (see

Figure 1e), where the photoactive layer are PTQ10:PY-IT blend, PM6:PY-IT blend, or PM6:PTQ10:PY-IT blend. The selection of polymer PY-IT as acceptor is due to its strong light absorption in NIR region and suitable electronic energy levels.[27] The binary all-PSCs based on PTQ10:PY-IT and PM6:PY-IT are fabricated with donor/acceptor weight ratio of 1.2:1.0 with a total concentration of 14 mg/mL in chloroform solution, 1.0% 1-chloronaphthalene (1-CN) as solvent additive, and thermal annealing at 95 °C for 5 min (**Tables S1**-**S2** in SI). The ternary all-PSCs based on PM6:PTQ10:PY-IT are fabricated with the same fabrication conditions (**Tables S3**-**S5** in SI) as that of the binary devices with carefully modifying the amount of PTQ10 (the optimal weight ratio of PM6:PTQ10:PY-IT is 1.0:0.2:1.0). The detailed device fabrication procedures are described in the Supporting Information.

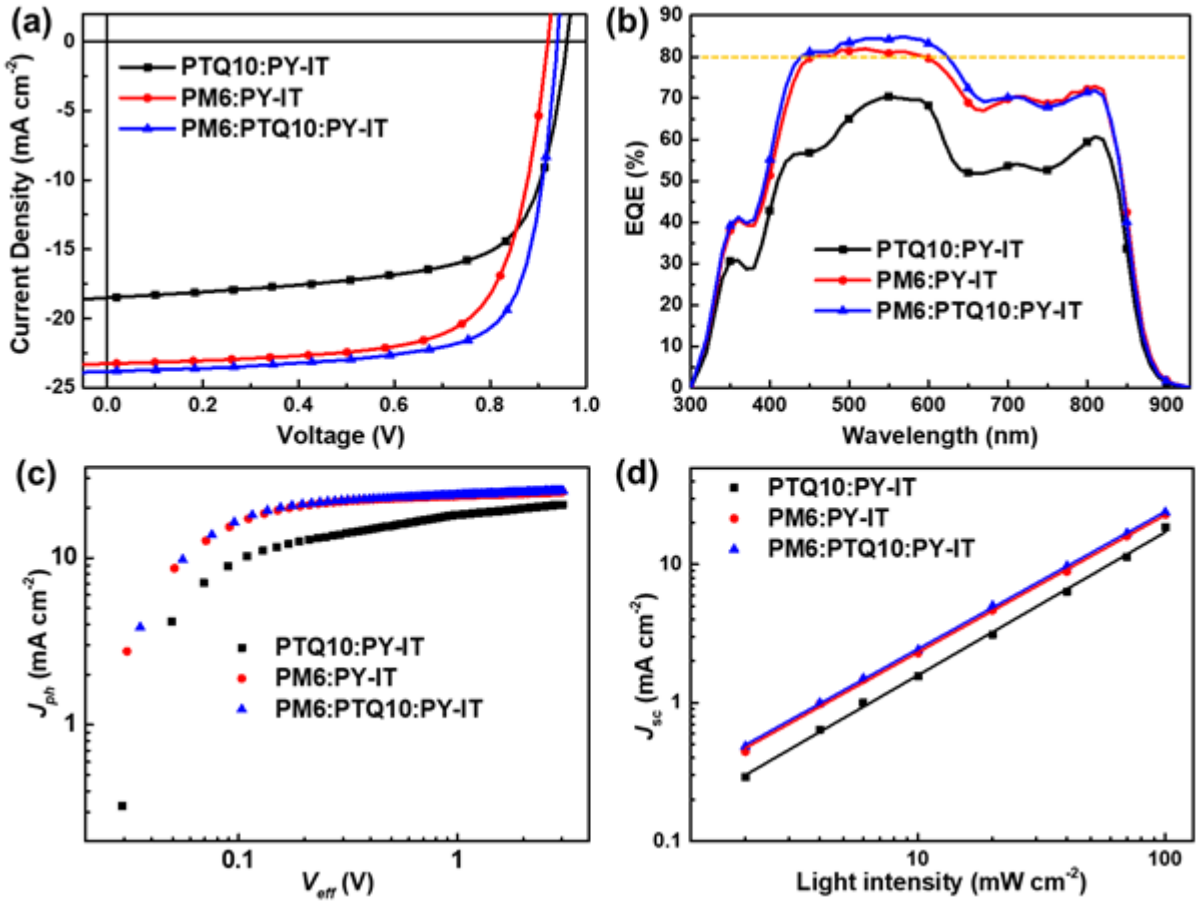

Figure 2. a) *J*-*V* curves of the optimal binary and ternary all-PSCs, under the illumination of AM 1.5G, 100 mW cm^{-2}. b) EQE spectra of the corresponding optimal binary and ternary all-PSCs. c) J_{ph} versus

V_{eff} of the optimal binary and ternary all-PSCs. d) Dependence of J_{sc} on P_{light} of the optimal binary and ternary all-PSCs.

Table 1. Photovoltaic performance parameters of the optimal binary and ternary all-PSCs under the illumination of AM 1.5G, 100 mW cm^{-2}.

Photoactive layer	V_{oc} (V)	J_{sc} (mA cm^{-2})	J_{SC}^{EQE} (mA cm^{-2})	FF (%)	PCE (%)
PTQ10:PY-IT (1.2:1.0)	0.96	18.51	17.83	68.16	12.11 (11.87 ± 0.22)[a]
PM6:PY-IT (1.2:1.0)	0.92	23.27	22.40	70.55	15.10 (14.91 ± 0.13)
PM6:PTQ10:PY-IT (1.0:0.2:1.0)	0.94	23.79	22.85	73.87	16.52 (16.28 ± 0.16)

[a]The average values are calculated from 10 devices.

Figure 2a shows the current density-voltage (*J-V*) curves of the optimal binary and ternary all-PSCs under the illumination of AM 1.5G, 100 mW cm^{-2}, and the corresponding photovoltaic performance parameters are summarized in **Table 1**. The binary device based on PTQ10:PY-IT exhibits a moderate PCE of 12.11%, with a higher V_{oc} of 0.96 V benefitted from the deeper HOMO energy level of the polymer donor PTQ10.[42,44] The optimal PM6:PY-IT based binary all-PSC demonstrates a higher PCE of 15.10% with a V_{oc} of 0.92 V, a J_{sc} of 23.27 mA cm^{-2}, and an FF of 70.55%, which are consistent with the reported results.[27] With the addition of the third component of polymer donor PTQ10, the PM6:PTQ10:PY-IT based ternary devices show obviously increased V_{oc} in the range of 0.93 to 0.95 V (**Table S3** in SI). Moreover, the addition of PTQ10 leads to improved FF in the range of 71.14% to 73.87% in comparison with the PM6:PY-IT based binary device, which might originate from the enhanced charge separation and transport in the photoactive layer. As a result, PCE of the

PM6:PTQ10:PY-IT (1.0:0.2:1.0) based ternary all-PSC is improved to as high as 16.52%. It is worth noting that, when the weight ratio of PTQ10 is increased to 0.3, PCE of the corresponding ternary device (PM6:PTQ10:PY-IT = 1.0:0.3:1.0) dramatically drops to 15.34% with relatively lower J_{sc} and FF, implying that morphology of the ternary blend photoactive layer is sensitive to the amount of PTQ10. The *J-V* curves of the ternary all-PSCs with different polymer weight ratios are shown in **Figures S2** in SI, and the corresponding photovoltaic performance parameters are listed in **Table S3** in SI.

To confirm and better understand the enhanced photovoltaic performance of the ternary all-PSCs, external quantum efficiency (EQE) spectra of the optimal binary and ternary all-PSCs are measured, as shown in **Figure 2b** and **Figure S3** in SI. It can be seen that both of the PM6:PY-IT based binary device and the PM6:PTQ10:PY-IT based ternary device exhibit broad photon response in the wavelength region of 350-850 nm with the maximum EQE values over 80%, indicating their remarkable photoelectric conversion efficiencies. Compared with the PM6:PY-IT (1.2:1.0) based binary device, the PM6:PTQ10:PY-IT (1.0:0.2:1.0) based ternary all-PSC presents enhanced photon response in the wavelength range from 450-700 nm, which is in accordance with the higher J_{sc} observed in the ternary device. Taking the film absorption spectra into consideration, the higher J_{sc} values of the ternary device can be ascribed to the enhanced molecular aggregation feature in the photoactive blend induced by the addition of polymer PTQ10. The current density values integrated (J_{SC}^{EQE}) from the EQE curves are 17.83, 22.40, and 22.85 mA cm^{-2} for the all-PSCs based on PTQ10:PY-IT, PM6:PY-IT, and PM6:PTQ10:PY-IT respectively, which are consistent well with the J_{sc} values obtained from the *J-V* curves within 5% mismatch, indicating the high reliability of the measured photovoltaic performance data.

Adding the third polymer component into the binary host blend will modify the microstructure of the interpenetrating network photoactive layer, thus affecting the exciton dissociation and charge

carrier recombination processes in the blend, and photovoltaic performance of the all-PSCs.[1,2] To investigate the exciton dissociation details of the three all-PSCs, the dependence of photocurrent density (J_{ph}) on effective voltage (V_{eff}) of the three devices are measured and the results are shown in **Figure 2c**. J_{ph} is defined as $J_{ph} = J_L - J_D$, where J_L and J_D are the current densities of the devices under illumination and in the dark, respectively. The V_{eff} ($V_{eff} = V_0 - V_{bias}$) is the difference between the voltage (V_0) when J_{ph} is zero and the applied voltage bias (V_{bias}). Thus, V_{eff} determines the electric field in the photoactive layer, and charge carriers quickly migrate to the electrodes as J_{ph} reaches a saturated state (J_{sat}) at a high V_{eff} ($V_{eff} \geq 2$ V), indicating that the maximum number of photogenerated excitons are dissociated into the free charge carriers and extracted by the corresponding electrodes.[45] Therefore, the exciton dissociation probability (P_{diss}) can be characterized by the J_{ph}/J_{sat} value. The P_{diss} values are measured to be 93.6%, 95.6%, and 96.3% for the all-PSCs based on PTQ10:PY-IT based, PM6:PY-IT based, and PM6:PTQ10:PY-IT, respectively. The higher P_{diss} value for the PM6:PTQ10:PY-IT based ternary device than the PM6:PY-IT based binary device indicates that the addition of PTQ10 promotes the processes of exciton dissociation and charge carrier collection in the device, which can account for the increased J_{sc} and FF in the ternary devices.

Then, the dependence of J_{sc} and V_{oc} on light intensity (P_{light}) are measured to estimate the charge carrier recombination behavior in all the three all-PSCs. The relationship between J_{sc} and P_{light} can be defined as $J_{sc} \propto (P_{light})^{\alpha}$, where α indicates the degree of bimolecular recombination, e.g., the α value should be 1 if all free charge carriers are extracted and collected at the corresponding electrodes without recombination. **Figure 2d** shows the plots of $\log(J_{sc})$ versus $\log(P_{light})$. The α values are measured to be 1.034, 0.991, and 0.994 for the devices based on PTQ10:PY-IT, PM6:PY-IT, and PM6:PTQ10:PY-IT, respectively. For the PM6:PY-IT based binary all-PSCs and the PM6:PTQ10:PY-IT based ternary all-PSCs, the α values are very close to 1 indicating that there is almost no bimolecular

recombination in the two devices, especially the latter. In addition, if there is no trap-assisted recombination and monomolecular recombination in the photoactive layer, the slope of the fitting straight line of V_{oc} versus ln(P_{light}) should be kT/q (where k is the Boltzmann constant, T is the Kelvin temperature, and q is the elementary charge). As shown in **Figure S4** in SI, the slopes of the fitting lines are 1.36 kT/q, 1.22 kT/q, and 1.18 kT/q for the devices based on PTQ10:PY-IT based, PM6:PY-IT based, and PM6:PTQ10:PY-IT, respectively. The results suggest that the trap-assisted recombination and monomolecular recombination are also suppressed in the PM6:PTQ10:PY-IT based ternary all-PSC with the addition of PTQ10. This results, together with the restrained bimolecular recombination and the improved exciton dissociation, indicates that the addition of PTQ10 induces the microscopic morphology of the photoactive layer of the ternary devices to the more desired texture, which is more conducive to charge separation and transport in the blend films. These results should be responsible for the increased J_{sc}, FF, and PCE of the ternary all-PSCs.

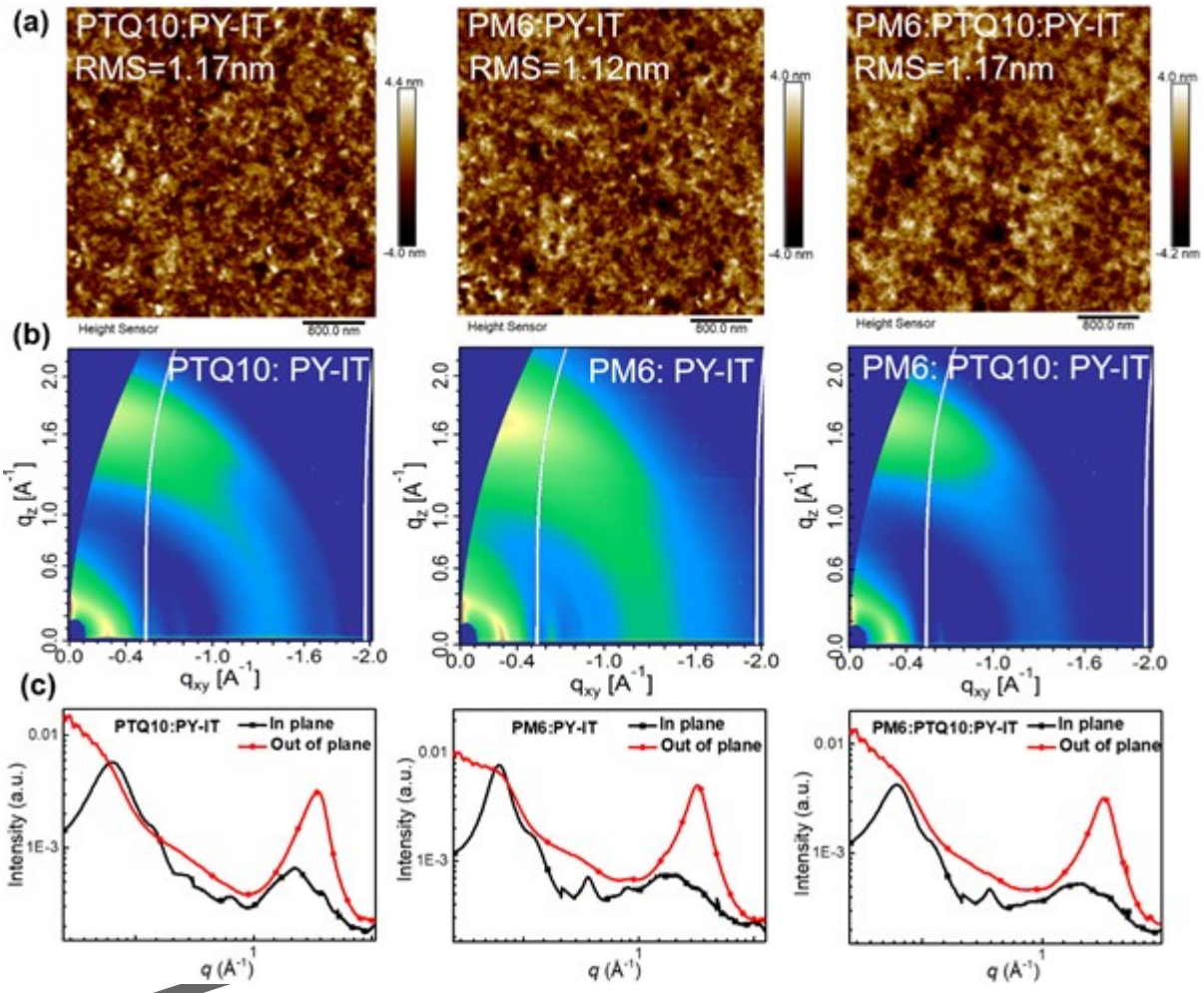

Figure 3. a) AFM height images of the three polymer blend photoactive layers. b) The 2D GIWAXS patterns of the three polymer blend photoactive layers. c) The in-plane and out-of-plane line cuts of the three polymer blend photoactive layers.

Table 2. The GIWAXS measurements data of the scattering vector *q*, π-π stacking distancce *d*, peak width Δ*q,* and coherence length (CL) of the neat and blend films.

Sample	*q* [010] (Å^{-1})	*d* [010] (Å)	Δ*q* [010] (Å^{-1})	CL [010] (Å)
PTQ10	1.77	3.55	0.222	28
PM6	1.72	3.66	0.321	20
PY-IT	1.62	3.89	0.346	18

PTQ10:PY-IT*	1.73	3.63	0.287	22
PM6:PY-IT*	1.66	3.77	0.302	21
PM6:PTQ10:PY-IT*	1.68	3.75	0.256	25

*One single peak fitting is used for the π-π contributions.

Morphology of the photoactive layer plays a critical role in determining the photovoltaic performance of the all-PSCs. Generally, the morphology featuring suitable nano-scale phase separation and ordered π-π molecular packing is beneficial for exciton dissociation on the donor/acceptor (D/A) interface and charge carrier transport in the photoactive layer, which is greatly conducive for obtaining high efficiency all-PSCs.[32,33] Here, we employ atomic force microscopy (AFM) and grazing incidence wide-angle X-ray diffraction (GIWAXS)[46] measurements, to probe the molecular packing and crystallinity features in the photoactive layer, for unveiling the impact of polymer PTQ10 on the microscopic texture of the photoactive blends as well as the photovoltaic performance of the devices. The results are shown in **Figure 3** and **Figure S5** in SI. From the AFM images (**Figure 3a**), the PM6:PY-IT based binary photoactive blend exhibits uniform and smooth surface morphologies with smaller root-mean-square (RMS) roughness value of 1.12 nm, indicating good miscibility between polymer donor and polymer accepter in the blend. With the addition of PTQ10, the RMS roughness value increases to 1.17 nm for the PM6:PTQ10:PY-IT ternary blend. Typically, the surface RMS roughness value of the photoactive layer is positively correlated with the molecular aggregation in the blend.[47] Thus, it is clear that the addition of PTQ10 induces an enhanced molecular aggregation in the photoactive blend, implying that the PM6:PTQ10:PY-IT ternary blend might possess better charge transport capability bacause the charge transportation through the overlapped π-orbital is the dominated charge carrier transport mechanism in the all-PSCs.

Figure S5 in SI and **Figure 3b**-**3c** show the GIWAXS measurement results of the neat polymer films and the polymer blend films. For the neat polymer films, the well-defined π-π stacking diffraction peaks ((010) peak) in the out-of-plane (OOP) direction are observed for the three polymers (**Figure S5** in SI), suggesting that the three polymers prefer face-on molecular orientation in the OOP direction in the films. The π-π stacking diffraction peaks for the polymers PTQ10, PM6, and PY-IT are located at 1.77, 1.72, and 1.62 $Å^{-1}$, corresponding to the π-π stacking distance of 3.55, 3.66, and 3.89 Å, respectively (**Table 2**). Their coherence lengths (CL) of π-π stacking in the OOP direction are 28 Å for PTQ10, 20 Å for PM6, and 18 Å for PY-IT, calculated from the Scherrer equation (CL = $2\pi K/\Delta q$, where K=1 is a shape factor and Δq is the full-width at half-maximum of the peak).[48] The PTQ10 film has the smallest π-π stacking distance (should be ascribed to the simplest molecular structure of PTQ10) and largest CL in the OOP direction, indicating the tightest and ordered molecular face-on packing among the three polymers. The closer and ordered molecular face-on packing of PTQ10 is beneficial for its efficient charge transport in the vertical direction of the substrate. The GIWAXS results of the blend films demonstrate microstructural features with the diffraction patterns contributed from the individual donor and acceptor components. Thus, as expected, the three blend films exhibit predominant face-on molecular packing orientation with well-defined π-π stacking diffraction peaks in the OOP direction (**Figure 3b-3c**). The π-π stacking diffraction peaks in the OOP direction for the PTQ10:PY-IT blend and the PM6:PY-IT blend are observed at 1.73 and 1.66 $Å^{-1}$ with the π-π stacking distance of 3.63 and 3.77 Å, respectively. With adding PTQ10 into the PM6:PY-IT binary host blend, the PM6:PTQ10:PY-IT ternary blend exhibits slightly decreased π-π stacking distance of 3.75 Å in the OOP direction. The slightly decreased π-π stacking distance should be attributed to two factors. One is that the polymer PTQ10 possesses smallest π-π stacking distance (3.55 Å) due to its simple molecular structure. Another is that the addition of PTQ10 might induce tighter molecular π-π stacking (polymers PM6 and/or PY-IT) in the ternary blend. Moreover, the CL

in the OOP direction for the ternary blend increased to 25 Å from 21 Å. Furthermore, the shape parameter η changes from 1 and 0.79 for the binaries, whereas the ternary blend is the most Guassian with η = 0.44 and the CL is likely limited by lattice parameter fluctuations rather than the paracrystallinity. These favorable changes indicate the improved molecular ordering that are beneficial to charge transport in the films, thus the PM6:PTQ10:PY-IT ternary blend should possess stronger charge transport capability and higher charge mobilities. This results together with the AFM results indicate that the addition of PTQ10 into the PM6:PY-IT blend optimizes the molecular packing and aggregate ordering in the films, resulting in the more ordered face-on molecular packing orientation in the OOP direction, which is conducive for charge transport and for obtaining higher J_{sc} and FF.

The hole mobilities (μ_h) and electron mobilities (μ_e) of the three polymer blend photoactive layers are measured through space-charge-limited current (SCLC) method to evaluate their charge transport properties, as shown in **Figure S6**-**S7** in SI. For the PM6:PY-IT binary blend, the μ_h and μ_e are measured to be 7.36×10^{-4} and 5.73×10^{-4} cm^2 V^{-1} s^{-1} with a μ_h/μ_e ratio of 1.28 (**Table S6** in SI). With the addition of PTQ10, the μ_h and μ_e of the PM6:PTQ10:PY-IT ternary blend increase to 7.86×10^{-4} and 6.81×10^{-4} cm^2 V^{-1} s^{-1} with a more balanced μ_h/μ_e ratio of 1.15, meaning more excellent charge transport properties of the ternary blend. Considering what have been discussed above, the highest PCE of 16.52% for the ternary all-PSC based on PM6:PTQ10:PY-IT is attributed to the increased V_{oc} of the device, the more efficient exciton dissociation, the minimal charge carrier recombination, and the better charge carrier transport in the photoactive layer.

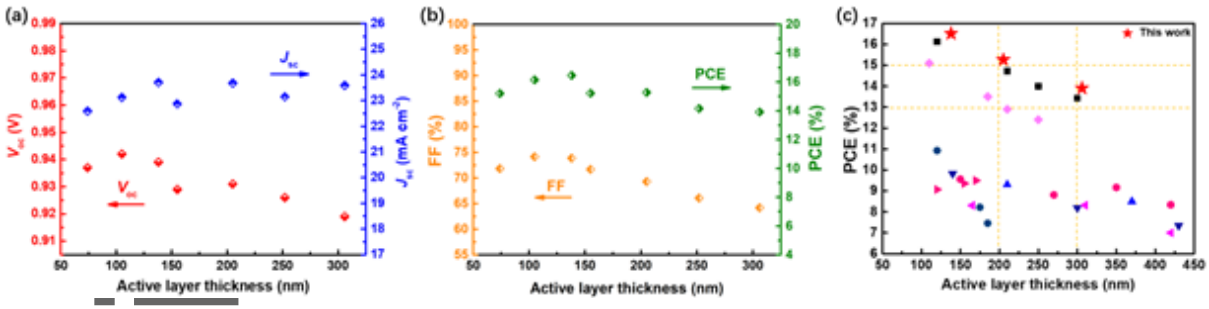

Figure 4. a) Plot of the V_{oc} and J_{sc} versus the photoactive layer thickness ranging from ~ 74 to ~ 306 nm. b) Plot of the FF and PCE versus the photoactive layer thickness ranging from ~ 74 to ~ 306 nm. c) Plot of the PCE values versus photoactive layer thickness of the high-efficiency all-PSCs with thick photoactive layer reported in literatures.

For realizing industrial application of the all-PSCs, it is crucial that their photovoltaic performance should possess high tolerance of the photoactive layer thickness.[49] Despite significant progress has been achieved for the all-PSCs with thin photoactive layer, the research on high-efficiency all-PSCs with thick photoactive layer is quite fewer. Here, we fabricated the PM6:PTQ10:PY-IT (1.0:0.2:1.0) based ternary all-PSCs with photoactive layer thickness ranging from ~ 74 to ~ 306 nm, to investigate the dependence of its photovoltaic performance on photoactive layer thickness. The results are shown in **Figure 4** and **Table S7** in SI. The V_{oc} values of the devices show relatively small fluctuations around 0.94 V when the photoactive layer thickness is in the range of ~ 74 to ~ 155 nm. While it shows a slightly decreasing trend as further increasing the photoactive layers thickness, which might be ascribed to the increased charge carrier recombination in the thicker blend films. For the J_{sc}, the gradually increasing values are observed with the increase of the photoactive layer thickness in the range of less than 150 nm, then the J_{sc} values change little at around 23~24 mA cm^{-2} with the further increase of the photoactive layer thickness, probably due to the trade-off between the increased light absorption and charge carrier recombination for the thicker photoactive layers. While the photoactive layer thickness significantly influences the FF values of the all-PSCs. The FF value of the

device with photoactive layer thickness of 105 nm shows the maximum value of 74.14%, and then it decreases with the further increase of the photoactive layer thickness. The reduced FF values should be related to the increased charge carrier recombination and increased series resistance of the devices with thick photoactive layer.[48] As a result, the highest PCE of 16.52% is obtained for the all-PSCs with the photoactive layer thickness of ~ 138 nm. Meanwhile, the high PCEs of 15.27% and 13.91% are achieved for the devices with the thicker photoactive layers of 205 nm and 306 nm respectively, which are the highest PCEs for the all-PSCs with the thick photoactive layer (**Figure 4c** and **Table S8** in SI). The result indicates that the high-performance ternary all-PSCs based on PM6:PTQ10:PY-IT with high tolerance of the photoactive layer thickness in the range of 100~300 nm is a promising candidate for industrial application.

3. Conclusion

In summary, we have successfully optimized the molecular packing and ordering of the aggregates in the photoactive layer of the all-PSCs based on PM6:PY-IT, by adding a small amount of low-cost polymer donor PTQ10 as the third component. The addition of PTQ10 in the ternary polymer blend induces a favourable morphological change with closer π-π stacking, improved CL, reduced paracrystallinity, and more ordered face-on molecular packing orientation in the vertical direction of substrate, which leads to improved exciton dissociation, reduced charge carrier recombination, and better charge transport capability of the devices. Moreover, the deeper HOMO energy level of the polymer donor PTQ10 than PM6 leads to increased V_{oc} of the ternary device. As a result, the all-PSC based on PM6:PTQ10:PY-IY demonstrates an impressive PCE of 16.52% with simultaneously enhanced V_{oc}, J_{sc}, and FF compared with its binary counterparts. In addition, the photovoltaic performance of the ternary devices exhibit high tolerance of the photoactive layer thickness in the

thickness range of ~ 70 to ~ 300 nm, with PCEs of 15.27% and 13.91% at photoactive layer thickness of ~ 205 nm and ~ 306 nm respectively, which are the highest PCEs for the all-PSCs with thick photoactive layer so far. The results demonstrate the importance of ternary blend strategy for improving the photovoltaic performance of the all-PSCs, and indicate the great potential of the PM6:PTQ10:PY-IT based ternary all-PSCs for future industrial application.

Conflict of Interest

The authors declare no conflict of interest.

Supporting Information

Supporting Information is available from the Wiley Online Library or from the author.

Acknowledgements

W. Z. and C. S. contributed equally to this work. This work was supported by the National Natural Science Foundation of China (Nos. 52103240, 51820105003, 21734008, and 61904181), the National Key Research and Development Program of China (No. 2019YFA0705900) funded by MOST, the Natural Science Foundation of Henan (No. 212300410284), and the Basic and Applied Basic Research Major Program of Guangdong Province (No. 2019B030302007). X-ray data acquisition and manuscript input by NCSU authors supported by ONR grant N000142012155. X-ray data were acquired at the Advanced Light Source, which was supported by the Director, Office of Science,

Office of Basic Energy Sciences, of the U.S. Department of Energy under Contract DE-AC02-05CH11231.

Received: ((will be filled in by the editorial staff))
Revised: ((will be filled in by the editorial staff))
Published online: ((will be filled in by the editorial staff))

References

[1] C. Lee, S. Lee, G.-U. Kim, W. Lee, B. J. Kim, *Chem. Rev.* **2019**, *119*, 8028-8086.

[2] G. Wang, F. S. Melkonyan, A. Facchetti, T. J. Marks, *Angew. Chem. Int. Ed.* **2019**, *58*, 4129-4142.

[3] Q. Burlingame, M. Ball, Y.-L. Loo, *Nat. Energy* **2020**, *5*, 947-949.

[4] S. Chen, S. Jung, H. J. Cho, N.-H. Kim, S. Jung, J. Xu, J. Oh, Y. Cho, H. Kim, B. Lee, Y. An, C. Zhang, M. Xiao, H. Ki, Z.-G. Zhang, J.-Y. Kim, Y. Li, H. Park, C. Yang, *Angew. Chem. Int. Ed.* **2018**, *57*, 13277-13282.

[5] Q. Fan, W. Su, S. Chen, W. Kim, X. Chen, B. Lee, T. Liu, U.A. Méndez-Romero, R. Ma, T. Yang, W. Zhuang, Y. Li, Y. W. Li, T.-S. Kim, L. Hou, C. Yang, H. Yan, D. Yu, E. Wang, *Joule* **2020**, *4*, 658-672.

[6] J. Du, K. Hu, L. Meng, I. Angunawela, J. Zhang, S. Qin, A. Liebman□Pelaez, C. Zhu, Z. Zhang, H. Ade, Y. Li, *Angew. Chem. Int. Ed.* **2020**, *59*, 15181-15185.

[7] J.-W. Lee, C. Sun, B. S. Ma, H. J. Kim, C. Wang, J. M. Ryu, C. Lim, T.-S. Kim, Y.-H.

Kim, S.-K. Kwon, B. J. Kim, *Adv. Energy Mater.* **2021**, *11*, 2003367.

[8] F. Peng, K. An, W. Zhong, Z. Li, L. Ying, N. Li, Z. Huang, C. Zhu, B. Fan, F. Huang, Y. Cao, *ACS Energy Lett.* **2020**, *5*, 3702-3707.

[9] H. Sun, B. Liu, Y. Ma, J. Lee, J. Yang, J. Wang, Y. Li, B. Li, K. Feng, Y. Shi, B. Zhang, D. Hang, H. Meng, L. Niu, B. J. Kim, Q. Zheng, X. Guo, *Adv. Mater.* **2021**, 2102635.

[10] H. Yu, S. Luo, R. Sun, I. Angunawela, Z. Qi, Z. Peng, W. Zhou, H. Han, R. Wei, M. Pan, A. M. H. Cheung, D. Zhao, J. Zhang, H. Ade, J. Min, H. Yan, *Adv. Funct. Mater.* **2021**, *31*, 2100791.

[11] R. Sun, W. Wang, H. Yu, Z. Chen, X. Xia, H. Shen, J. Guo, M. Shi, Y. Zheng, Y. Wu, W. Yang, T. Wang, Q. Wu, Y. (Michael) Yang, X. Lu, J. Xia, C. J. Brabec, H. Yan, Y. Li, J. Min, *Joule* **2021**, *5*, 1548-1565.

[12] T. Jia, J. Zhang, K. Zhang, H. Tang, S. Dong, C.-H. Tan, X. Wang, F. Huang, *J. Mater. Chem. A* **2021**, *9*, 8975-8983.

[13] H. Fu, Y. Li, J. Yu, Z. Wu, Q. Fan, F. Lin, H. Y. Woo, F. Gao, Z. Zhu, A. K.-Y. Jen, *J. Am. Chem. Soc.* **2021**, *143*, 2665-2670.

[14] Q. Fan, H. Fu, Q. Wu, Z. Wu, F. Lin, Z. Zhu, J. Min, H. Y. Woo, A. K.□Y. Jen, *Angew. Chem. Int. Ed.* **2021**, *60*, 15935-15943.

[15] F. Liu, L. Zhou, W. Liu, Z. Zhou, Q. Yue, W. Zheng, R. Sun, W. Liu, S. Xu, H. Fan, L. Feng, Y. Yi, W. Zhang, X. Zhu, *Adv. Mater.* **2021**, 2100830.

[16] C. Li, J. Zhou, J. Song, J. Xu, H. Zhang, X. Zhang, J. Guo, L. Zhu, D. Wei, G. Han, J.

Min, Y. Zhang, Z. Xie, Y. Yi, H. Yan, F. Gao, F. Liu, Y. Sun, *Nat. Energy* **2021**, *6*, 605-613.

[17] Y. Cui, Y. Xu, H. Yao, P. Bi, L. Hong, J. Zhang, Y. Zu, T. Zhang, J. Qin, J. Ren, Z. Chen, C. He, X. Hao, Z. Wei, J. Hou, *Adv. Mater.* **2021**, 2102420.

[18] S. Bao, H. Yang, H. Fan, J. Zhang, Z. Wei, C. Cui, Y. Li, *Adv. Mater.* **2021**, 2105301.

[19] Z.-G. Zhang, Y. Yang, J. Yao, L. Xue, S. Chen, X. Li, W. Morrison, C. Yang, Y. Li, *Angew. Chem. Int. Ed.* **2017**, *56*, 13503-13507.

[20] Y. Meng, J. Wu, X. Guo, W. Su, L. Zhu, J. Fang, Z.-G. Zhang, F. Liu, M. Zhang, T. P. Russell, Y. Li, *Sci. China Chem*. **2019**, *62*, 845-850.

[21] Z.-G. Zhang, Y. Li, *Angew. Chem. Int. Ed.* **2021**, *60*, 4422.

[22] H. Yao, F. Bai, H. Hu, L. Arunagiri, J. Zhang, Y. Chen, H. Yu, S. Chen, T. Liu, J. Y. L. Lai, Y. Zou, H. Ade, H. Yan, *ACS Energy Lett.* **2019**, *4*, 417-422.

[23] J. Yuan, Y. Zhang, L. Zhou, G. Zhang, H.-L. Yip, T.-K. Lau, X. Lu, C. Zhu, H. Peng, P. A. Johnson, M. Leclerc, Y. Cao, J. Ulanski, Y. Li, Y. Zou, *Joule* **2019**, *3*, 1140-1151.

[24] T. Jia, J. Zhang, W. Zhong, Y. Liang, K. Zhang, S. Dong, L. Ying, F. Liu, X. Wang, F. Huang, Y. Cao, *Nano Energy* **2020**, *72*, 104718.

[25] W. Wang, Q. Wu, R. Sun, J. Guo, Y. Wu, M. Shi, W. Yang, H. Li, J. Min, *Joule* **2020**, *4*, 1070-1086.

[26] H. Sun, H. Yu, Y. Shi, J. Yu, Z. Peng, X. Zhang, B. Liu, J. Wang, R. Singh, J. Lee, Y. Li, Z. Wei, Q. Liao, Z. Kan, L. Ye, H. Yan, F. Gao, X. Guo, *Adv. Mater.* **2020**, *32*, 2004183.

[27] Z. Luo, T. Liu, R. Ma, Y. Xiao, L. Zhan, G. Zhang, H. Sun, F. Ni, G. Chai, J. Wang, C. Zhong, Y. Zou, X. Guo, X. Lu, H. Chen, H. Yan, C. Yang, *Adv. Mater.* **2020**, *32*, 2005942.

[28] Q. Fan, Q. An, Y. Lin, Y. Xia, Q. Li, M. Zhang, W. Su, W. Peng, C. Zhang, F. Liu, L. Hou, W. Zhu, D. Yu, M. Xiao, E. Moons, F, Zhang, T. D. Anthopoulos, O. Inganäs, E. Wang, *Energy Environ. Sci.* **2020**, *13*, 5017-5027.

[29] J. Du, K. Hu, J. Zhang, L. Meng, J. Yue, I. Angunawela, H. Yan, S. Qin, X. Kong, Z. Zhang, B. Guan, H. Ade, Y. Li, *Not. Commun.* **2021**, *12*, 5264.

[30] H. Lee, C. Park, D. H. Sin, J. H. Park, K. Cho, *Adv. Mater.* **2018**, *30*, 1800453.

[31] Q. He, W. Sheng, M. Zhang, G. Xu, P. Zhu, H. Zhang, Z. Yao, F. Gao, F. Liu, X. Liao, Y. Chen, *Adv. Energy Mater.* **2021**, *11*, 2003390.

[32] J. Lv, H. Tang, J. Huang, C. Yan, K. Liu, Q. Yang, D. Hu, R. Singh, J. Lee, S. Lu, G. Li, Z. Kan, *Energy Environ. Sci.* **2021**, *14*, 3044-3052.

[33] S. Kwon, J. K. Park, J. Kim, G. Kim, K. Yu, J. Lee, Y.-R. Jo, B.-J. Kim, H. Kang, J. Kim, H. Kim, K. Lee, *J. Mater. Chem. A* **2015**, *3*, 7719-7726.

[34] Q. Zhao, H. Lai, H. Chen, H. Li, F. He, *J. Mater. Chem. A* **2021**, *9*, 1119-1126.

[35] D. Yang, F. C. Löhrer, V. Körstgens, A. Schreiber, S. Bernstorff, J. M. Buriak, P. Müller-Buschbaum, *ACS Energy Lett.* **2019**, *4*, 464-470.

[36] X. Wang, L. Zhang, L. Hu, Z. Xie, H. Mao, L. Tan, Y. Zhang, Y. Chen, *Adv. Funct. Mater.* **2021**, *31*, 2102291.

[37] S. J. Lou, N. Zhou, X. Guo, R. P. H. Chang, T. J. Marks, L. X. Chen, *J. Mater. Chem. A*

2018, *6*, 23805-23818.

[38] X. Liu, X. Li, L. Wang, J. Fang, C. Yang, *Nanoscale* **2020**, *12*, 4945-4952.

[39] X. Xu, K. Feng, L. Yu, H. Yan, R. Li, Q. Peng, *ACS Energy Lett.* **2020**, *5*, 2434-2443.

[40] K. Hu, J. Du, C. Sun, C. Zhu, J. Zhang, J. Yao, Z. Zhang, Y. Wan, Z. Zhang, L. Meng, Y. Li, *Energy Fuels* **2021**, *35*, 19045-19054.

[41] T. Liu, T. Yang, R. Ma, L. Zhan, Z. Luo, G. Zhang, Y. Li, K. Gao, Y. Xiao, J. Yu, X. Zou, H. Sun, M. Zhang, T. A. D. Pena, Z. Xing, H. Liu, X. Li, G. Li, J. Huang, C. Duan, K. S. Wong, X. Lu, X. Guo, F. Gao, H. Chen, F. Huang, Y. F. Li, Y. L. Li, Y. Cao, B. Tang, H. Yan, *Joule* **2021**, *5*, 914-930.

[42] C. Sun, F. Pan, H. Bin, J. Zhang, L. Xue, B. Qiu, Z. Wei, Z.-G. Zhang, Y. Li, *Nat. Commun.* **2018**, *9*, 743.

[43] M. Zhang, X. Guo, W. Ma, H. Ade, J. Hou, *Adv. Mater.* **2015**, *27*, 4655-4660.

[44] C. Sun, F. Pan, S. Chen, R. Wang, R. Sun, Z. Shang, B. Qiu, J. Min, M. Lv, L. Meng, C. Zhang, M. Xiao, C. Yang, Y. Li, *Adv. Mater.* **2019**, 1905480.

[45] C. Sun, S. Qin, R. Wang, S. Chen, F. Pan, B. Qiu, Z. Shang, L. Meng, C. Zhang, M. Xiao, C. Yang, Y. Li, *J. Am. Chem. Soc.* **2020**, *142*, 1465-1474.

[46] A. Hexemer, W. Bras, J. Glossinger, E. Schaible, E. Gann, R. Kirian, A. MacDowell, M. Church, B. Rude, H. Padmore, *J. Phys.: Conf. Ser.* **2010**, *247*, 012007.

[47] D. Hu, Q. Yang, H. Chen, F. Wobben, V. M. Le Corre, R. Singh, T. Liu, R. Ma, H. Tang, L. J. A. Koster, T. Duan, H. Yan, Z. Kan, Z. Xiao, S. Lu, *Energy Environ. Sci.* **2020**, *13*,

2134-2141.

[48] Y. Yang, Z.-G. Zhang, H. Bin, S. Chen, L. Gao, L. Xue, C. Yang, Y. Li, *J. Am. Chem. Soc.* **2016**, *138*, 15011-15018.

[49] X. Gu, Y. Zhou, K. Gu, T. Kurosawa, Y. Guo, Y. Li, H. Lin, B. C. Schroeder, H. Yan, F. Molina-Lopez, C. J. Tassone, C. Wang, S. C. B. Mannsfeld, H. Yan, D. Zhao, M. F. Toney, Z. Bao, *Adv. Energy Mater.* **2017**, *7*, 1602742.

16.52% efficiency all-PSC is achieved by morphology control of the photoactive layer through adding low-cost polymer donor PTQ10 into the PM6:PY-IT blend. Meanwhile, the ternary devices exhibit high tolerance of the photoactive layer thickness, with high PCEs of 15.27% and 13.91% at photoactive layer thickness of ~ 205 nm and ~ 306 nm respectively.

Wenqing Zhang, Chenkai Sun*, Indunil Angunawela, Lei Meng, Shucheng Qin, Liuyang Zhou, Shaman Li, Hongmei Zhuo, Guang Yang, Zhi-Guo Zhang, Harald Ade*, and Yongfang Li*

16.52% Efficiency All-Polymer Solar Cells with High Tolerance of the Photoactive Layer Thickness